Adhesion properties of a structural etch stop material for use in multilayer electronic wiring structures

Ruud A. Haring, Sharon L. Nunes, Richard P. McGouey, and Eileen A. Galligan
IBM Research Division, Thomas J. Watson Research Center, P.O. Box 218, Yorktown Heights, New York 10598

Willi Volksen, James L. Hedrick, and Jeff Labadie
IBM Research Division, Almaden Research Center, 650 Harry Road, San Jose, California 95120

(Received 10 August 1994; accepted 12 December 1994)

A thermally stable copolymer of a polyimide and a dianiline terminated polydimethylsiloxane has been developed for use as a structural oxygen etch barrier material in high performance multilayer electronic wiring structures. We report on the preparation of the etch barrier material and on investigations of the etch stop and adhesion properties of this material. Studies on the effects of adhesion-promoting plasma treatments are supported by x-ray photoelectron spectroscopy (XPS) and Rutherford backscattering spectrometry (RBS) data. Before plasma treatment, it is observed that the siloxane component segregates to the surface. After either an O_2 reactive ion etch treatment or H_2O plasma exposure, the unusual XPS charging effects are interpreted as a surface layer containing two distinct phases: the etched polyimide fraction and a partial overlayer of a carbon containing SiO_2.

I. INTRODUCTION

Interconnect structures based on polymeric dielectrics with imbedded thin film metal wiring have many advantages for high performance electronic packaging, such as the thin film module employed in the high end models of the IBM ES/9000 series mainframes.[1–3]

Some alternative schemes for fabricating such a structure have been discussed in Ref. 4. If the wiring channels of a given wiring plane inside the structure are defined using reactive ion etching (RIE) of the polyimide dielectric, then an etch stop layer is preferably used to protect underlying polyimide. Such a layer, made of a suitable oxygen etch barrier material, then allows for a reasonable amount of overetching, thus providing a manufacturable process window (see Fig. 1).

It should be noted that in such a scheme the etch stop material will remain in the wiring structure. The material, therefore, should have a low dielectric constant, very good thermal stability, durability, and good adhesion properties to the polyimide above and below. Moreover, as shown in Ref. 4, good gap-filling properties of the etch stop material are very useful if the metallization of the wiring channels is done by lift-off. Such an etch stop material has recently been developed by incorporation of polydimethylsiloxane (PMDS) segments into a thermally stable, high T_g polyimide, such as pyromellitic dianhydride-oxydianiline (PMDA-ODA) (Fig. 2).

In this article, we report on the etch properties under O_2 RIE conditions and on the adhesion properties of this material. In particular, since the siloxane and polyimide fractions of the copolymer are immiscible, the siloxane fraction will tend to segregate to the surface. This necessitates a surface treatment to ensure adhesion to the polyimide layer on top. The effects of such surface treatments are investigated using surface analysis techniques.

II. EXPERIMENTAL

A. Formulation of the etch stop material

An etch stop material with the required properties of low dielectric constant, very good thermal stability, and durability has recently been developed by incorporation of polydimethylsiloxane (PMDS) segments into pyromellitic dianhydride-oxydianiline (PMDA-ODA) (Fig. 2). The dimethylsiloxane segments are based on aminophenyl-terminated dimethylsiloxane oligomers with reactivity akin to traditional aromatic diamines utilized in the synthesis of polyimides as well as improved thermal stability in comparison to γ-aminopropyl-terminated siloxane oligomers.[5] In addition, by changing the classical polyimide precursor synthesis, i.e., dianhydride/diamine reaction to form a poly(amic acid), to one which utilizes a diamine/dialkylester diacyl chloride reaction to form a poly(amide alkyl ester), it is possible to isolate the soluble polyimide precursor and extract any homopolymer contamination as well as residual siloxane cyclics.[6] Further advantages of the latter synthetic approach are realized by the improved solubility of the diacyl chloride monomer, in particular, the meta-diester diacyl chloride isomer, which makes it possible to retain a completely homogeneous poly-

 © 1995 Materials Research Society

https://doi.org/10.1557/JMR.1995.1028 Published online by Cambridge University Press

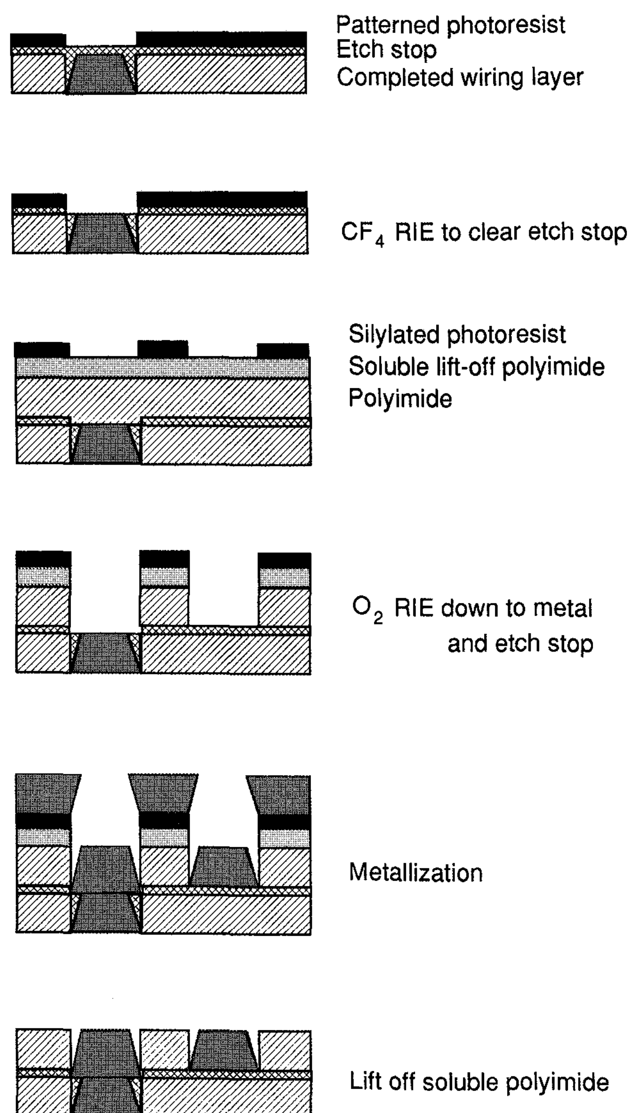

FIG. 1. Schematic buildup of the multilayer wiring structure with etch stop.[4]

merization reaction. In this fashion, well-characterized segmented block copolymers consisting of polyimide and poly(dimethylsiloxane) units have been prepared.

B. Synthesis of poly(*p*-oxydiphenylene-meta-diethyl pyromellitamide-co-dimethylsiloxane)

132.12 g (0.660 mole) of freshly sublimed 4,4′-oxydianiline (ODA) and 2.7 L of distilled N-methylprrolidone (NMP) were charged into a 10 L resin kettle equipped with a mechanical stirrer, liquid addition funnel, and argon bubbler. Next, 266.35 g (0.213 mole) of bis(4-aminophenyl)dimethylsiloxane oligomer ($\overline{M}_n = 1250$), 175.0 g (1.73 mole) of distilled triethylamine, followed by 2.7 L of distilled tetrahydrofuran (THF) were added. The homogeneous solution was then cooled externally via ice/water for at least 30 min to bring the internal temperature to ca. 5°C. At this point, 300.0 g (0.864 mole) of meta-diethyl pyromellitate diacyl chloride dissolved in 400 mL of dry tetrahydrofuran was added slowly via the liquid addition funnel over a period of approximately 2 h with vigorous stirring and maintaining the reaction temperature at 5–10 °C. Once addition was complete, the polymerization mixture was stirred for another 6 h and then 9.0 g (0.0263 mole) of sym-methyl phthalate anhydride endcapper was added. Stirring was continued for an additional 9 h and then the reaction mixture was precipitated into ca. 10 gal of de-ionized (DI) water using a blender. The precipitate was filtered, washed on the filter with more DI water, and resuspended in 3 gal of DI water and stirred overnight. This extraction was followed by another water extraction, a methanol/water = 80/20 extraction, and finally an isopropanol extraction before being dried *in vacuo* at 50 °C for 48 h. The overall yield of desired product was 589 g (92.7%). Elemental analysis indicated a silicon content of 10.7 wt.%, and neutron activation analysis yielded the following ionic contaminants: Na 7.9 ppm, Cl 11.4 ppm, and K $<$ 1 ppm.

The resulting material is hereafter referred to as "PAETE-RIE", from PolyAmic EThyl Ester-Reactive Ion Etch barrier. From the molecular weight distribution of the siloxane oligomers, it can be inferred that in Fig. 2 $\langle m \rangle \sim 15$, and from the silicon content that $\langle n \rangle / \langle m \rangle$ is about 2.

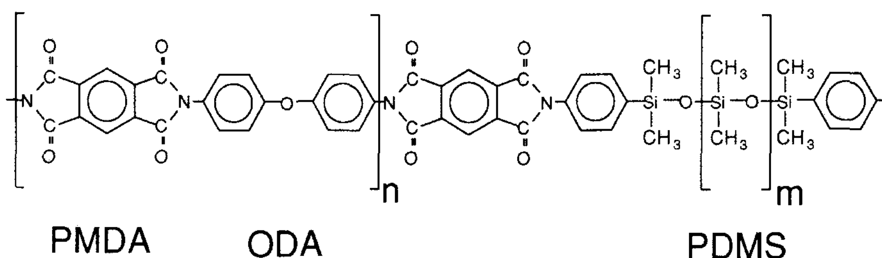

FIG. 2. Chemical structure of a thermally stable copolymer of pyromellitic dianhydride-oxydianiline (PMDA-ODA) and polydimethylsiloxane (PMDS).

https://doi.org/10.1557/JMR.1995.1028 Published online by Cambridge University Press

C. Etch stop properties

Blanket samples of biphenyltetracarboxylic dianhydride-*p*-phenylenediamine (BPDA-PDA polyimide, Dupont 5811) and PAETE-RIE etch stop material were prepared on glass ceramic substrate. A PlasmaTherm 2460 etch tool was used for determining the etch rates of both polyimide and etch stop. A HeNe laser interferometer was used to optically monitor the etch rates as a function of time.

In the O_2 RIE process, the actual gas mixture used was 2% CF_4/98% O_2. The 2% CF_4 addition to the oxygen was found to eliminate the "RIE grass" commonly observed when using pure O_2 in a silylated photoresist O_2-RIE transfer process.[7]

D. Peel tests

Since the etch-stop material remains as a permanent part of the multilayer structures (Fig. 1), it is critical that the adhesion is sufficient to withstand all subsequent processing steps. The adhesion of PAETE-RIE to polyimide was investigated (case a), as well as the adhesion of polyimide to PAETE-RIE (b).

Several samples were prepared for peel testing as follows:

(1) Chromium was evaporated onto a clean silicon wafer.

(2) A1100 adhesion promoter (0.1% in water) was spin applied.

(3) BPDA-PDA polyimide was spin applied to a thickness of 3 μm after full cure (350 °C).

(4) The polyimide was surface treated for 5 min in either a water plasma or O_2 RIE: O_2 RIE in a PlasmaTherm 2460 at 20 mTorr and 600 W; water plasma in a modified PlasmaTech tool at 180 mTorr, 50 W, 13.56 MHz, plasma etch (PE) mode.

(5) A gold release layer was applied to one end of the wafer sample.

(6) PAETE-RIE etch stop was spin applied and cured to 350 °C. Final thickness was 1 μm.

(7) PAETE-RIE layer was surface treated for 5 min in either a water plasma or O_2 RIE, as above.

(8) A gold release layer was applied to one end of the wafer sample.

(9) BPDA-PDA polyimide (DuPont 5811) was spin applied to a thickness of 10 μm after full cure (350 °C).

(10) 2.5 μm strips were scribed on the sample and peel tested[8] in the 90° mode at 4.55 in./min peel speed using an Instron instrument, modified to accept the peel fixture.

Note: only the release layer at step 5 (case a) or 8 (b) was applied, depending on the interface being examined. For control samples, the interface being examined was not treated (i.e., step 4 or 7 omitted).

E. XPS analysis

For x-ray photoelectron spectroscopy (XPS) analysis, 1.2 μm etch stop films were deposited on Si substrates, cured to 350 °C in a nitrogen atmosphere, and exposed to either the O_2/2% CF_4 RIE plasma or a H_2O plasma for various lengths of time (0.5, 1, 2, 4, 8, and 16 min). Without any further treatment, the resulting films have been analyzed using angle resolved XPS (Leybold EA-11 analyzer, VSW x-ray source, using the Mg K_α and Al_α lines). The fixed angle between x-ray source and detector is 50°; to obtain depth resolution the sample was tilted with its normal in the plane of detector and x-ray source. The detection angles (0° and 60°) are given with respect to the sample normal. The spectra presented here were taken with 50 eV pass energy. Because of the analysis in "as-received" condition and because of moderate vacuum conditions, some adventitious carbon and oxygen contamination of the top layer is likely.

The linearity of the analyzer was checked immediately after these experiments. The binding energies (BE) of various Ag, Cu, and Au peaks from a test sample agreed over a 1000 eV range with literature values[9] with a linearity to within 3×10^{-4}.

F. RBS analysis

In the Rutherford backscattering spectroscopy (RBS) analysis, identical samples as in the XPS analysis above were exposed to a beam of 200 keV H^+ ions. These ions scatter from the atoms they encounter, and thereby lose energy in the elastic collision. This energy loss is related to scattering angle and mass of the collision partner. Furthermore, the H^+ ions lose energy through inelastic processes while penetrating the surface, both on their way in (before the elastic scattering event) and on their way out after scattering. Therefore, the energy loss is related to the depth of the scattering atom as well as its mass.[10] Backscattered ions were collected in a toroidal electrostatic analyzer, yielding simultaneous scattering angle and energy resolved data.[11,12] With 55° incident angle (with respect to surface normal) and nominally 70° exit angle, the total scattering angle used was around $180 - 55 - 70 = 55°$. For these noncrystalline samples, there is no extra information in the scattering angle. Therefore, the data were summed over a small range of exit angles (±0.8°) to get better statistics in the energy spectra. The beam spot (about 0.1×2 mm) was shifted over the surface many times per spectrum, to minimize radiation damage.

III. RESULTS

A. Etch stop properties

For a material to perform as an acceptable etch stop in our process, it was estimated that an etch-rate ratio

https://doi.org/10.1557/JMR.1995.1028 Published online by Cambridge University Press

(of polyimide to etch stop) of 5 : 1 would be desirable. This would allow a broad process window for manufacturing the wiring layer. A high-percentage overetch is frequently implemented as part of the "standard" process, to compensate for geometry-related variations in etch rate. A 5 : 1 etch rate ratio in our structure would allow a 40–50% overetch of the BPDA-PDA polyimide if needed.

Various RIE conditions (power/pressure) were evaluated in the PlasmaTherm 2460 tool to optimize the etching of the polyimide pattern, while still maintaining adequate etch resistance of the PAETE-RIE etch stop. Etch rates of the PAETE-RIE in the 2% CF_4/98% O_2 plasma ranges from 100 Å/min (500 W, 200 mTorr) to 225 Å/min (600 W, 20 mTorr). The etch rate of the BPDA-PDA ranged from 1000 Å/min to 1600 Å/min under similar conditions.

The conditions finally chosen for etching in the PlasmaTherm 2460 were 600 W, 20 mTorr, 100 sccm, 2% CF_4/98% O_2 using a graphite electrode. Under these conditions, the BPDA-PDA etches at 1100 Å/min and the PAETE-RIE etches at 200 Å/min.

B. Peel test results

Processing of multilayer thin films requires multiple thermal cycles and exposure to solvents at several steps in the process. The structure may also be subjected to mechanical planarization steps.

Since two test structures had delaminated between the etch stop and polyimide, it was first believed that the adhesion at these interfaces was marginal. One substrate had delaminated during planarization and another during a rework process where a significant area of the PAETE-RIE etch stop had been exposed to hot (85 °C) N-methylpyrrolidone (NMP).

This prompted an investigation of the adhesion properties of both the PAETE-RIE interfaces: PAETE-RIE to (on top of) BPDA-PDA (case a), and BPDA-PDA to PAETE-RIE (case b): see Table I.

TABLE I. BPDA-PDA/PAETE-RIE /BPDA-PDA peel strength data as a function of surface treatment.

Sample (treatment)[a]	ES[b] from BPDA (g/mm)	BPDA from ES (g/mm)
Control	2–3	2–3
1 (O_2/NMP)	40, 40, 37	50, 55, 55
2 (O_2)	39, 42	55, 55
3 (H_2O/NMP)	40, 40	51, 55, 56
4 (H_2O)	39, 40	45, 46, 51, 52, 43, 42, 42

[a]O_2 RIE conditions: 20 mTorr, 600 W, 5 min; H_2O plasma conditions: 180 mTorr, 50 W, 5 min.
[b]ES stands for the PAETE-RIE (etch stop) material.

TABLE II. BPDA-PDA/PAETE-RIE /BPDA-PDA peel strength data after samples were immersed in NMP and baked.

Sample	ES[a] from BPDA (g/mm)	BPDA from ES (g/mm)
1	36	52, 53, 52
2	35	52, 50
3	43, 42	53, 52
4	45, 43	51

[a]ES stands for the PAETE-RIE (etch stop) material.

For each interface, samples 1 and 2 were O_2 reaction ion etched and samples 3 and 4 were surface treated with a water plasma. Samples 1 and 3 were immersed in hot NMP and baked with the PAETE-RIE layer exposed, before the BPDA-PDA overcoat was applied. Samples 2 and 4 had no solvent exposure before the BPDA-PDA overcoat was applied.

To see whether a rework-type operation would affect the adhesion properties, all samples were once more immersed in hot NMP and baked subsequent to these initial peel tests. After this treatment the peel strengths tabulated in Table II were measured.

Based on previous experience, these peel strength values indicate sufficient adhesion properties for manufacturability of a multilayer wiring structure. Furthermore, immersion of the peel test samples into NMP between coatings and/or after initial peel testing showed little change (5–10%) from the samples not exposed to the solvent. The adhesion data also indicated little or no difference between the O_2 RIE and water plasma surface treatments for the PAETE-RIE/polyimide combination. In the absence of a plasma surface treatment, however, the adhesion of PAETE-RIE to polyimide or polyimide to PAETE-RIE was poor. In fact, without surface modification, both materials showed very poor wetting on each other.

C. XPS analysis

The effects of the adhesion promoting plasma treatments on PAETE-RIE have been investigated using XPS and RBS. Both techniques are sensitive to the top few monolayers of the sample surface. With XPS, both survey and detail spectra were taken. The detail spectra are shown in Fig. 3 and 4.

XPS analysis of PAETE-RIE samples treated with a H_2O plasma yielded the following noteworthy features (see Fig. 3): (i) In the first 30 s of plasma treatment, there is a substantial uptake of oxygen in the top layer, measured with respect to the Si signal. (ii) With respect to Si, all other signals show quick depletion in the top layer [C, N, and O (after the first 30 s)].

In contrast, for samples treated with the 98% O_2/2% CF_4 plasma we observe the following (Fig. 4): (i) The total oxygen/silicon ratio in the layer is more stable. The

https://doi.org/10.1557/JMR.1995.1028 Published online by Cambridge University Press

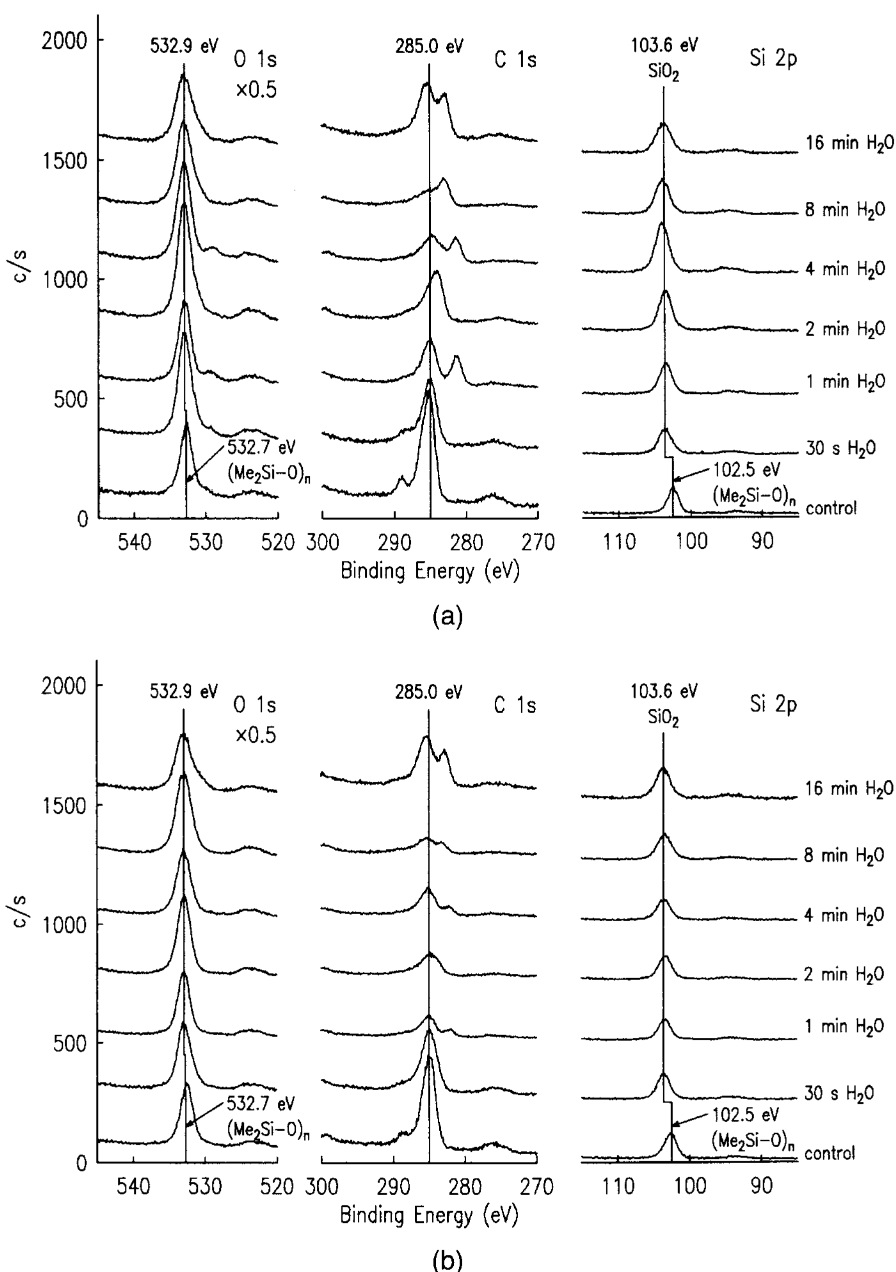

FIG. 3. XPS spectra of H_2O plasma-treated etch stop material: (a) 0° detection angle; (b) 60° detection angle.

increase from about 6 to 7.5 in the relative XPS signal corresponds to an increase from about 1.5 to 1.75 in the O/Si atom ratio.[9] (ii) The C/Si ratio drops by a factor of 4 within the first 30 s, and is more stable afterward. (iii) The N/Si ratio drops precipitously as well. (iv) A small incorporation of F is visible, on the order of 1%. (v) The stoichiometry in the top surface layers stabilizes at roughly Si : C : O = 4 : 5 : 7 (with intensity correction factors[9] applied). As mentioned above, (part of) the visible carbon may be adventitious.

As far as peak positions and peak shapes are concerned, both plasma treatments show rather similar results (Figs. 3 and 4) with a few notable differences described below.

In the survey spectra the peak separation between Si 2*p* and O 1*s* has been measured. In the untreated (control) sample this separation is 430.1 ± 0.1 eV. In all treated samples (both O_2 and H_2O plasma treated, for all exposure times) it is 429.5 ± 0.1 eV. The former value is perfectly consistent with literature values for $(Me_2SiO)_n$ (polydimethylsiloxane),[13] the latter with SiO_2.[14] This means that in both the H_2O and the O_2 plasma the dimethylsiloxane is converted to essentially SiO_2 within 30 s under the conditions given.

https://doi.org/10.1557/JMR.1995.1028 Published online by Cambridge University Press

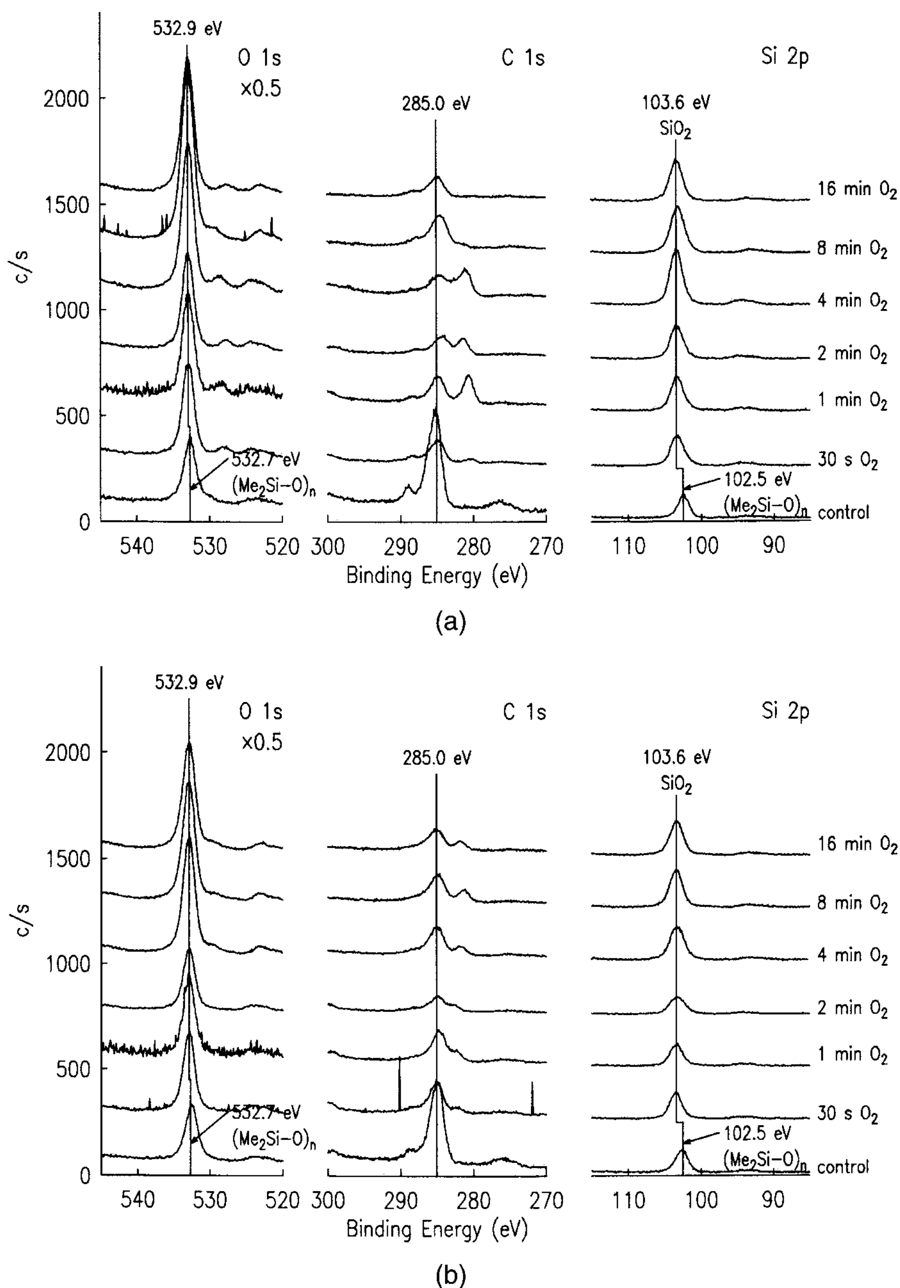

FIG. 4. XPS spectra of O_2 RIE treated etch stop material: (a) 0° detection angle; (b) 60° detection angle.

Since the samples were subject to charging during irradiation, we have used the above result for charge compensation: assuming the top layer in the control (untreated) samples to be mainly dimethylsiloxane, we used the O 1*s* peak at a binding energy (BE) of 532.7 eV as a charge reference, following Ref. 13. For dimethylsiloxane, the Si 2*p* peak then falls at about 102.6 eV, and the C 1*s* at 285.0 eV, the customary value for aromatic/aliphatic carbon.[13] Our results (bottom spectra in Figs. 3 and 4) are in very good agreement with this.

An argument can be made that for dimethylsiloxane the C 1*s* binding energy is reduced to 284.2 eV, due to the chemical shift of carbon adjacent to silicon.[15] This would bring Si 2*p* to 101.8 eV (in better agreement with the values for "Si^{2+}" in silicon suboxides[14]) and O 1*s* to 531.9 eV. However, this argument has been ignored in the subsequent literature on XPS of dimethylsiloxane.[9,13,16] The debate on the absolute values of the dimethylsiloxane binding energies is relevant to the shift (charge compensation) of the spectrum as a whole. Our conclusion that the control spectra represent dimethylsiloxane, however, is based only on the binding energy difference between the Si 2*p* and O 1*s* peaks, and is independent of the overall shift.

https://doi.org/10.1557/JMR.1995.1028 Published online by Cambridge University Press

In the plasma-treated samples (all other spectra of Figs. 3 and 4) we have shifted the spectra to have the O 1*s* peaks coincide at 532.9 eV, consistent with the value for thin SiO_2.[14]

In all spectra, the Si 2*p* signal (Figs. 3 and 4) is a single peak, without any features, except a slight peak broadening observed with continuing plasma exposure. We suspect that this is "smearing" due to differential charging. The peak widths of all signals show this broadening trend with processing time.

The major part of the C 1*s* peak (Figs. 3 and 4) is at/around 285.0 eV (after charge referencing to O 1*s* as described above). This is the value expected for graphitic, aliphatic, and aromatic carbon. However, almost all C 1*s* spectra (except control and 30 s H_2O treated samples), and many O 1*s* spectra as well, have pronounced features (shoulders or even separate peaks) at the right-hand (low binding energy) side, shifted by −3 to −4 eV with respect to the main peak. Usually these "extra" peaks are more pronounced looking under 0° than under 60°. In some samples this peak is even dominant; see C 1*s* for H_2O/8 min/0° [Fig. 3(a)], and for O_2/1 and 4 min/0° [Fig. 4(a)]. These low binding energy features in C 1*s* and O 1*s* are a charging phenomenon, rather than chemical shifts, as could be ascertained by flood electron gun irradiation (which made the peaks reversibly collapse; see Fig. 5) and by varying x-ray source to sample distance (hence x-ray flux).

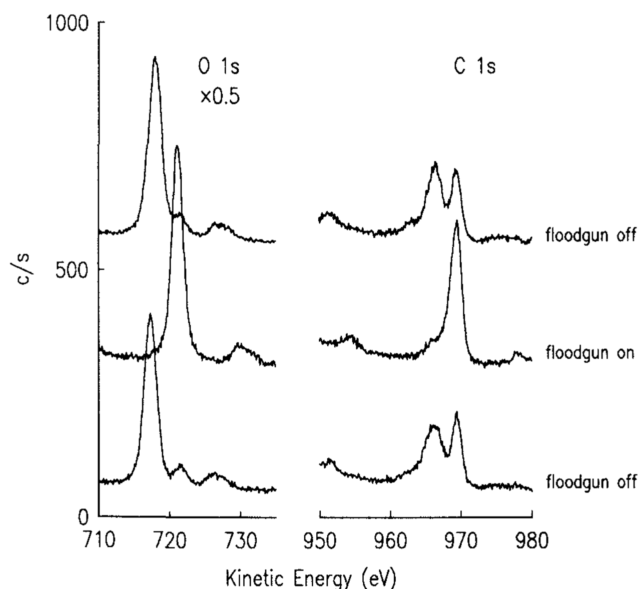

FIG. 5. Effect of electron flood gun irradiation on XPS peak shapes and positions for C 1*s* (from 1 min O_2 plasma-treated sample) and O 1*s* (from 2 min O_2 plasma-treated sample). Spectra were taken consecutively in the sequence flood gun off (bottom trace), flood gun on (middle trace), and flood gun off (top trace) for either sample. Spectra taken for 0° detection angle. No corrections applied for sample charging.

Overall, in doing this series of experiments, we did not keep irradiation intensity under close control. X-ray source to sample distances and x-ray source operating conditions varied within a certain range. Any trends in the low binding energy (right-hand side) features of Figs. 3 and 4 may therefore be due to experimental artifact. In particular, we cannot ascribe significance to the differences in peak shapes between 0° and 60° exit angles, since with the sample tilt, the angle and distance to the x-ray source were varied.

We may conclude, however, that these "extra" features indicate the existence of two different phases on the surface. These phases are very discrete: they maintain a steady potential difference of 3–4 V under our x-ray irradiation conditions. This also means that the surface conductivity between both phases is very small. Differential charging within either phase is only minor (peak broadening). Si (mostly as a C-containing SiO_2 layer) is present in only one phase (single unsplit peak), whereas C and O are incorporated in both phases. The visible carbon is distributed up to 50%–50% between the phases; of the visible oxygen, 90–100% is associated with the Si phase.

Notice that we don't see the dual-phase charging in the untreated control sample. This leads to two possible inferences: (i) If the peak splitting is taken as an indication of lateral copolymer phase separation, then the charging properties of the siloxane fraction and polyimide fraction of the untreated polymer are similar, whereas after plasma treatment the charging properties of the treated polyimide and the to-SiO_2-converted siloxane are very dissimilar; or (ii) There is no lateral copolymer phase separation, but the SiO_2 in the treated samples only partially covers the surface. This may be due to stress-induced cracking or flaking off. At present, we tend to favor the latter possibility (Fig. 6).

From the flood gun experiments in Fig. 5, we conclude that the SiO_2 phase, which contains the majority of the O 1*s* signal, charges up by +3 to +4 V when the flood gun is off. The "extra" peaks in the other phase appear to be relatively unshifted under irradiation with or without flood gun. However, since for Figs. 3 and 4 the binding energy scale was defined with respect to the O 1*s* signal in the SiO_2 phase (as if the peaks of the O 1*s* signals in Fig. 5 were all lined up), the "extra"

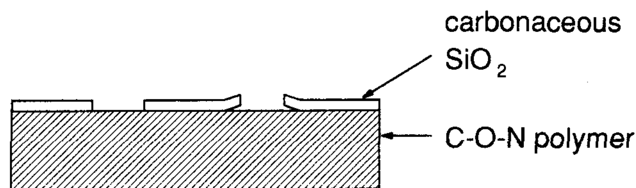

FIG. 6. Schematic of plasma-treated surface, consistent with XPS observations.

https://doi.org/10.1557/JMR.1995.1028 Published online by Cambridge University Press

peaks in Figs. 3 and 4 artificially appear at unnaturally low binding energies.

In Figs. 3 and 4 the control sample shows a feature at the high binding energy (left-hand) side of the main C 1*s* peak, shifted by +3.8 to 4.0 eV. This is ascribed to >C=O (carbonyl) from the polyimide fraction. Its signal is smaller than expected for PMDA-ODA, but this is explained by the additional C in the dimethylsiloxane and adventitious carbon. In all plasma-treated samples the carbonyl feature is weakened (on top of the overall carbon loss). The weakening is especially pronounced in the H_2O treated samples, where it is visible as a separate peak only in the 30 s treated sample, looking at 0° [Fig. 3(a)]. In the O_2 treated samples it is distinguishable in almost all 0° spectra [Fig. 4(a)]. This carbonyl feature is associated with the SiO_2 phase (since it is the charge reference). Within this phase, we may interpret the 0° spectra as looking "deep" and the 60° spectra as looking "shallow". If we assume that the carbonyl is indicative of the polyimide part of the etch stop material, then it looks as if it is under a top SiO_2 layer. That this feature can be observed implies that the original siloxane overlayer and processed SiO_2 overlayer thickness is of the order of the inelastic mean free path λ. For C 1*s* photoelectrons λ is estimated at about 8 ± 3 monolayers[17] or 12 ± 5 Å (assuming a monolayer to be defined by the average bond length of aromatic C–C, C–N, and Si–O, all about 1.5 Å).

Finally, the SiO_2-like top surface layer can be removed with an HF dip: see Fig. 7. After a short HF dip, the XPS spectra are consistent with a PMDA-like polymer, with a trace of (probably buried) silicon.

We believe that Fig. 6 represents the simplest surface configuration that is consistent with all these obser vations, although undoubtedly the real surface morphology may be more complicated, e.g., roughened.

D. RBS analysis

Figure 8(a) shows the backscattered energy spectrum of 200 keV protons on a PAETE-RIE control sample (untreated). The arrows indicate the expected position of protons that are elastically scattered from various elements if these were at a surface position.

It is seen that the surface in enriched in Si. The Si peak starts not quite at the surface, which may be due to some adventitious carbon and oxygen (which are seen at the very surface). The Si peak is about 1 keV wide, corresponding to about 2.6×10^{15} Me_2SiO groups/cm^2 for this scattering geometry, assuming this stoichiometry for the very surface layer. An area integration yields about $1.8 \times 10^{15}/cm^2$ for this peak. For a rather loosely packed surface such as Si or SiO_2, there are about 7×10^{14} atoms/cm^2 in a surface monolayer, so the peak width found would correspond to about 3 monolayers of siloxane on the surface (more if the siloxane is less densely packed).

Behind the surface peak, we see that the siloxane concentration falls back to about half the surface value for at least 10 monolayers, before the Si signal drowns in the oxygen and carbon signals.

Figure 8(b) shows the spectra of an etch stop sample that was treated for 4 min with a H_2O plasma. We see that the spectrum is now dominated by Si and O, and that the C level is very much less than in Fig. 8(a). Assuming SiO_2 as the medium, we calculate that the first 3.5 keV energy loss of the Si peak (from the Si edge to the O edge) corresponds to at least 1.5×10^{16} SiO_2 groups/cm^2, i.e., about 20 monolayers. The Si concentration tapers off only slowly over this visible range. The SiO_x layer may therefore well extend deeper.

Furthermore, we see some heavy metal contamination, consisting of two contributions: one consistent with a heavy metal such as Mo, another consistent with a

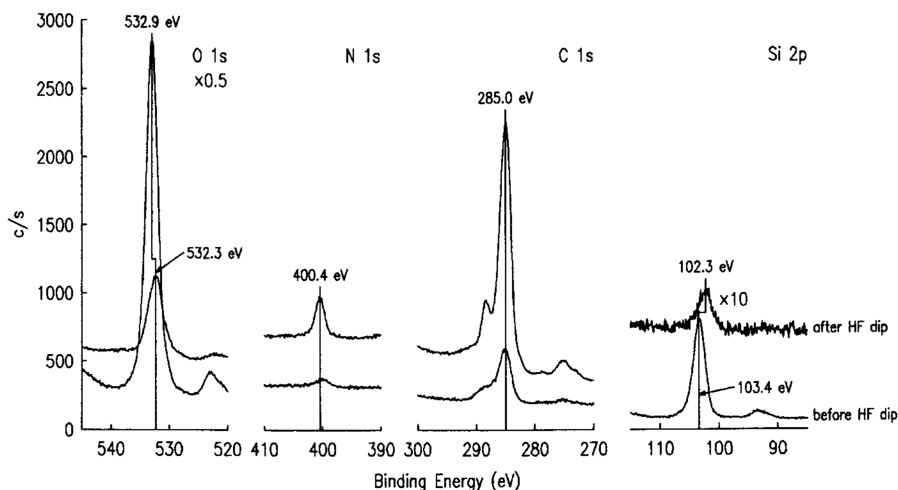

FIG. 7. XPS spectra for a 4 min H_2O plasma-treated sample before and after a dip in HF. Spectra taken for 0° detection angle.

https://doi.org/10.1557/JMR.1995.1028 Published online by Cambridge University Press

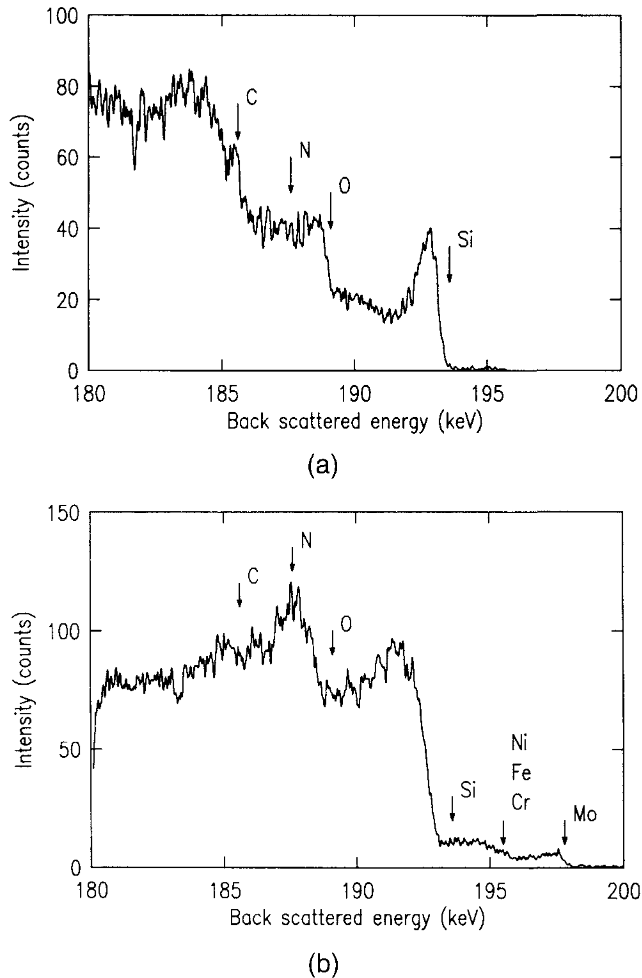

FIG. 8. RBS spectra taken with 200 keV H^+ ions of the etch stop material: (a) control sample; (b) sample treated for 4 min with a H_2O plasma.

lighter transition metal such as Fe, Ni, or Cr. RBS is very sensitive to heavy contaminations, since the scattering cross section is proportional to Z^2 (Z = atomic number). Mass resolution in this range is poor, however, so that the above identifications point only to the region of the periodic system where the contamination can be found. This contamination may result from sputtered stainless steel from the chamber walls of the plasma system.

IV. CONCLUSIONS

We have formulated, synthesized, and tested PAETE-RIE, a thermally stable copolymer of polyimide and dimethylsiloxane, for use as a structural etch stop layer in high performance multilayer electronic packaging structures. We identified the plasma conditions for a 5:1 O_2 RIE etch rate ratio between BPDA-PDA polyimide and PAETE-RIE. Adhesion between BPDA-PDA and PAETE-RIE requires that the interface is pretreated with a short O_2 RIE or water plasma step. The effects of these treatments on PAETE-RIE have been investigated using XPS and RBS. With these techniques, we clearly observe segregation of the siloxane component to the surface before plasma treatment. The siloxane ends up occupying about three top monolayers.

After either O_2 RIE or H_2O plasma exposure, we see a splitting of the XPS spectrum, which suggests that the surface layer is made up of two distinct phases, one of which is mostly a C-containing SiO_2. With O_2 RIE treatment we see carbonyl "shining through" in this phase. This is consistent with the idea that we have a partial coverage with a very thin (order 10 Å) carbonaceous SiO_2 layer, through which we see an underlying C–O–N polymer. Furthermore, a small amount (of the order of 1%) of F is incorporated in the top layer with the O_2/2% CF_4 RIE plasma treatment.

After a H_2O plasma treatment, the converted layer is substantially thicker than with O_2 RIE. With a H_2O plasma treatment, the SiO_x dominates for at least 20 monolayers, and may very well extend deeper. Apparently the H_2O plasma treatment has etched away most of the carbon to a considerable depth.

The conversion of the top layer due to plasma exposure takes place for the most part within 30 s under the given conditions. It is being investigated whether such a short treatment (or a "softer" exposure) is already sufficient to get adequate adhesion characteristics to subsequent polyimide layers.

Further efforts are underway to understand the mechanism of phase separation, to reduce the copolymer phase segregation by improved formulation, and to gain a better understanding of the adhesion promoting surface treatments.

ACKNOWLEDGMENTS

D. B. Ashbery assisted in the construction of the XPS equipment. W. S. Graham and D. J. Hunt assisted with SEM analysis, S. R. Kasi with exploratory surface treatments, and M. Copel and R. M. Tromp accommodated us on the RBS spectrometer. N. J. Chou, J. M. Baker, D. D. Dimilia, F. Bozso, J. E. Heidenreich, and J. R. Paraszczak are acknowledged for stimulating discussions, assistance, and support.

REFERENCES

1. E. E. Davidson, P. W. Hardin, G. A. Katopis, M. G. Nealon, and L. L. Wu, *IEEE Proc. 41st Electron. Comp. & Technol. Conf.* (1991), p. 50.
2. R. R. Tummala, H. R. Potts, and S. Ahmed, *IEEE Proc. 41st Electron. Comp. & Technol. Conf.* (1991), p. 682.
3. T. F. Redmond, C. Prasad, and G. A. Walker, *IEEE Proc. 41st Electron. Comp. & Technol. Conf.* (1991), p. 689.
4. J. Paraszczak, J. Cataldo, E. Galligan, W. Graham, R. McGouey, S. Nunes, R. Serino, D. Y. Shih, E. Babich, A. Deutsch, G. Kopcsay, R. Goldblatt, D. Hofer, J. Labadie, J. Hedrick, C. Narayan, K. Saenger, J. Shaw, V. Ranieri, J. Ritsko, L. Rothman,

https://doi.org/10.1557/JMR.1995.1028 Published online by Cambridge University Press

W. Volksen, J. Wilczynski, D. Witman, and H. Yeh, *IEEE Proc. 41st Electron. Comp. & Technol. Conf.* (1991), p. 362.

5. J.L. Hedrick, T.P. Russell, S. Swanson, D. Hofer, and W. Volksen, IBM Techn. Disclosure Bull. **37** (2A), 371 (1994).
6. W. Volksen, D.Y. Yoon, and J.L. Hedrick, IEEE Trans. Compon. Hybrids Manuf. Technol. **15** (1), 107 (1992).
7. C. Cunningham, in *Proc. 8th Symp. Plasma Processing,* edited by G.S. Mathad and D.W. Hess (Electrochemical Society, Pennington, NJ, 1990), Vol. 90–14, p. 759.
8. J. Kim, K.S. Kim, and Y.H. Kim, J. Adhesion Sci. Technol. **3** (3), 175 (1989).
9. C.D. Wagner, W.M. Riggs, L.E. Davis, J.F. Moulder, and G.E. Muilenberg, *Handbook of X-ray Photoelectron Spectroscopy* (Perkin-Elmer PHI, Eden Prairie, MN, 1979).
10. J.F. van der Veen, Surf. Sci. Rep. **5**, 199 (1985).
11. R.M. Tromp, H.H. Kersten, E. Granneman, F.W. Saris, R. Koudijs, and W.J. Kilsdonk, Nucl. Instrum. Methods B **4**, 155 (1984).
12. R.M. Tromp, M. Copel, M.C. Reuter, M. Horn-von Hoegen, J. Speidell, and R. Koudijs, Rev. Sci. Instrum. **62**, 2679 (1991).
13. J.A. Gardella, Jr., S.A. Ferguson, and R.L. Chin, Appl. Spectrosc. **40** (2), 224 (1986).
14. F.J. Grunthaner and P.J. Grunthaner, Mater. Sci. Rep. **1**, 65 (1986).
15. R.C. Gray, J.C. Carver, and D.M. Hercules, J. Electron. Spectrosc. Rel. Phen. **8**, 343 (1976).
16. C.D. Wagner, D.E. Passoja, H.F. Hillery, T.G. Kinisky, H.A. Six, W.T. Jansen, and J.A. Taylor, J. Vac. Sci. Technol. **21** (4), 933 (1982).
17. M.P. Seah, in *Practical Surface Analysis,* edited by D. Briggs and M.P. Seah (John Wiley, New York, 1983), Chap. 5.

https://doi.org/10.1557/JMR.1995.1028 Published online by Cambridge University Press